

## GLAUBER MONTE-CARLO PROGRAM FOR NICA/MPD AND CBM EXPERIMENTS

*A. S. Galoyan*<sup>1</sup>, *V. V. Uzhinsky*

Joint Institute for Nuclear Research, Dubna

A program code widely applied at RHIC and LHC for calculations of geometrical properties of nucleus–nucleus interactions is adapted for NICA/MPD and CBM energies. A parameterization of  $pp$ -elastic scattering amplitude earlier proposed by the authors and valid at  $\sqrt{s} \geq 3$  GeV is used for the setting of the nucleon–nucleon collision profile. An approach well-known in physics of low and intermediate energies is used for a determination of nuclear parameters. The code is enlarged by a possibility to account for the Gribov inelastic screening.

Программа, широко применяемая на RHIC и LHC для вычислений геометрических характеристик ядро-ядерных взаимодействий, адаптирована для экспериментов NICA/MPD и CBM. Для задания профиль-функции нуклон-нуклонных соударений используется параметризация, ранее предложенная авторами и справедливая при  $\sqrt{s} \geq 3$  ГэВ. Для определения ядерных параметров используется подход, широко известный в физике низких и промежуточных энергий. Программа расширена возможностью учета грибовского неупругого экранирования.

PACS: 25.75.-q; 25.75.Ag; 24.10.Lx; 02.70.Uu

The Glauber Monte-Carlo simulations [1] have become a basic tool in the analysis of relativistic heavy-ion collisions. The approach is mainly used at experimental studies for a determination of multiplicities of participating nucleons ( $N_{\text{part}}$ ) or multiplicities of binary nucleon–nucleon collisions ( $N_{\text{bin}}$ ) at a given centrality class<sup>2</sup>. The quantities are needed for a quantification of the particle production and the jet quenching effect in the created hot deconfinement matter. As known, the quark–gluon plasma is produced in high-energy nucleus–nucleus interactions. Conditions of its creation are not known exactly, and the NICA/MPD and CBM experiments are aimed to study them in detail at sufficiently low energies ( $\sqrt{s_{NN}} \leq 10$  GeV). Thus, an extension of the Glauber calculations into low-energy domain is required.

---

<sup>1</sup>E-mail: galoyan@lpub01.jinr.ru

<sup>2</sup>A connection between  $N_{\text{part}}$ ,  $N_{\text{bin}}$  and experimental measurements used for a centrality definition depends on many circumstances (see, for example, [2]): acceptance of a setup, energy of collisions, particle identification, and so on. Thus, it is very often assumed that for estimations of general geometrical properties of interactions it is quite sufficient to study dependencies of the quantities on impact parameter.

Last decade it was experimentally observed that there is a strong correlation between azimuthal anisotropy of particle production and azimuthal anisotropy of interaction region predicted by the Glauber approach. This found its explanation in the framework of the hydrodynamical model [3] at the assumption that the quark–gluon plasma is an ideal liquid! One can expect that the property will be changed at low energies, at the creation of a mixed phase. To distinguish the change, one needs estimations of the anisotropy of the interaction region at low energies.

The aim of our paper is the extension of the Glauber Monte-Carlo simulations into low-energy domain.

Cross section of new particle production in nucleus–nucleus interactions is given in the Glauber approximation [4] by the well-known expression:

$$\sigma_{AB}^{\text{prod}} = \sigma_{AB}^{\text{tot}} - \sigma_{AB}^{\text{el}} - \sigma_{AB}^{\text{q.el}} = \int d^2b \left\{ 1 - \prod_{i=1}^A \prod_{j=1}^B (1 - p_{ij}(\mathbf{b} - \mathbf{s}_i + \tau_j)) \right\} \times \\ \times |\psi_A(\mathbf{r}_1, \dots, \mathbf{r}_A)|^2 |\psi_B(\mathbf{t}_1, \dots, \mathbf{t}_B)|^2 \prod_{i=1}^A d^3r_i \prod_{i=1}^B d^3t_i, \quad (1)$$

where  $A$  and  $B$  are mass numbers of the nuclei;  $\mathbf{b}$  is the impact parameter;

$$p_{ij}(\mathbf{b}) = C_i C_j \gamma(\mathbf{b}) + C_i C_j \gamma^*(\mathbf{b}) - (C_i C_j)^2 \gamma(\mathbf{b}) \gamma^*(\mathbf{b});$$

$\gamma(\mathbf{b})$  is an amplitude of elastic nucleon–nucleon scattering in the impact parameter representation;  $C_i$  is a shower enhancement coefficient in the vertex of pomeron–nucleon interaction;  $\{\mathbf{s}_i\}$ ,  $i = 1, 2, \dots, A$  and  $\{\tau_j\}$ ,  $j = 1, 2, \dots, B$  are sets of coordinates of nucleons of  $A$  and  $B$  nuclei in the impact parameter plane;  $\mathbf{r}_i = (\mathbf{s}_i, z_i)$ ;  $\mathbf{t}_i = (\tau_i, \zeta_i)$ ;  $\psi_A$  and  $\psi_B$  are wave functions of the nuclei in the ground states. At  $C_i = 1$  one has the standard Glauber expression. At  $C_i \neq 1$  the Gribov inelastic screenings are taken into account. At this, each nucleon can be in an “active” state with a probability  $1/C$  and  $C_i = C$ , or in a “passive” state with a probability  $1 - 1/C$  and  $C_i = 0$ .

Equation (1) can be rewritten in a form where each term of the expansion can be interpreted as a cross section of processes with fixed multiplicity of nucleon–nucleon collisions:

$$\sigma_{AB}^{\text{prod}} = \int d^2b \left\{ \sum_{i=1}^A \sum_{j=1}^B \frac{p_{ij}(\mathbf{b} - \mathbf{s}_i + \tau_j)}{1 - p_{ij}(\mathbf{b} - \mathbf{s}_i + \tau_j)} \prod_{k=1}^A \prod_{l=1}^B (1 - p_{kl}(\mathbf{b} - \mathbf{s}_k + \tau_l)) + \right. \\ \left. + \frac{1}{2} \sum_{i=1, j=1}^A \sum_{k=1}^B \frac{p_{ik}(\mathbf{b} - \mathbf{s}_i + \tau_k)}{1 - p_{ik}(\mathbf{b} - \mathbf{s}_i + \tau_k)} \frac{p_{jk}(\mathbf{b} - \mathbf{s}_j + \tau_k)}{1 - p_{jk}(\mathbf{b} - \mathbf{s}_j + \tau_k)} \times \right. \\ \left. \times \prod_{l=1}^A \prod_{m=1}^B (1 - p_{lm}(\mathbf{b} - \mathbf{s}_l + \tau_m)) + \dots \right\} \times \\ \times |\psi_A(\mathbf{r}_1, \dots, \mathbf{r}_A)|^2 |\psi_B(\mathbf{t}_1, \dots, \mathbf{t}_B)|^2 \prod_{i=1}^A d^3r_i \prod_{i=1}^B d^3t_i. \quad (2)$$

For example, the first term is a cross section of processes with one inelastic nucleon–nucleon collision. The second term is a cross section of processes with two inelastic nucleon–nucleon collisions, and so on.

A complexity of Eqs. (1) and (2) prevents their analytical evaluation at a realistic choice of the scattering amplitude and nuclear densities with an exception  $A, B \leq 4$ . Thus, it was proposed in papers [5,6] to use Monte-Carlo averaging methods for the aim. This direction found its continuation in papers [7, 1, 8]. Especially, in paper [1] a program code was proposed, which uses modern computational tools — the ROOT system [9]. The code is intensively used in experiments at high energies, and is called “Glauber Monte Carlo”. Though, the code is not free from some drawbacks: the profile of inelastic nucleon–nucleon collisions is chosen in a simplified form ( $p_{ij}(\mathbf{b}) = \theta(r_{NN} - |\mathbf{b}|)$ ),  $r_{NN} = \sqrt{\sigma_{NN}^{\text{in}}/\pi}$ , a set of allowed nuclei is strongly restricted. These mean that one needs to point out, working with the code, a cross section of inelastic nucleon–nucleon collisions at a given energy of the collisions, and nuclei from a defined list. Some drawbacks of the code were erased in paper [8].

Recently, we have proposed [10–12] the following parameterization of the nucleon–nucleon elastic scattering amplitude which can be used in the Glauber calculations:

$$\gamma(b) = A_1 \left\{ \frac{1}{1 + e^{(b-\tilde{R})/d}} + \frac{1}{1 + e^{-(b+\tilde{R})/d}} - 1 \right\} - i\rho A_1 \frac{\tilde{R}^2/2 + \pi^2 d^2/6}{\tilde{R}d} \times \\ \times \left\{ \frac{e^{-(b-\tilde{R})/d}}{[1 + e^{-(b-\tilde{R})/d}]^2} + \frac{e^{-(b+\tilde{R})/d}}{[1 + e^{-(b+\tilde{R})/d}]^2} \right\} - i \frac{A_2}{2\pi B_2 \cdot 25.64} e^{-b^2/(2B_2 \cdot 25.64)}, \quad (3)$$

$$\tilde{R} = R + (0.07 + d + 0.2d^2) e^{-1.2R/d}, \quad (4)$$

$$A_1 = 1.077 - 0.175 e^{-0.001s^{0.5}} + 0.45/s^{0.25}, \quad (5)$$

$$R = 0.9/s^{0.25} + 0.053 \ln(s) \text{ [fm]}, \quad d = 0.379 - 0.26/s^{0.25} \text{ [fm]}, \quad (6)$$

$$\rho = 0.135 - \frac{3}{\sqrt{s}} + \frac{4}{s} + \frac{80}{s^3}, \quad (7)$$

$$A_2 = 1.77 \cdot 10^{-4} [\ln(s/225)]^2 + 0.05/s \text{ [fm}^2\text{]}, \quad (8)$$

$$B_2 = 0.283 \ln(s) + 30/s - 0.75 \text{ [(GeV/c)}^{-2}\text{]}. \quad (9)$$

The real part of the amplitude (3) is the symmetrized Fermi distribution. The imaginary part of the amplitude, which is small at high energies, has rather a complicated form due to usage of dispersion relations in differential forms. The last term of the amplitude is needed for a description of nucleon–nucleon elastic scattering at large momentum transfers ( $|t| > 1.75 \text{ (GeV/c)}^2$ ). The parameterization allows one to describe rather well experimental data on differential cross sections of proton–proton elastic scattering at  $\sqrt{s} \geq 3 \text{ GeV}$  [11].

Important structure elements of Eqs. (1) and (2) are squared modules of the nuclear wave functions in the ground states. Very often they are represented as

$$|\psi_A(\mathbf{r}_1, \dots, \mathbf{r}_A)|^2 = \left[ \prod_{i=1}^A \rho_A(\mathbf{r}_i) \right] \delta \left( \frac{1}{A} \sum_{i=1}^A \mathbf{r}_i \right). \quad (10)$$

Usually, at Monte-Carlo simulations the nucleon coordinates are sampled independently of each other according to the  $\rho_A$  distribution. After that the coordinates are redefined

as  $\mathbf{r}_i \rightarrow \mathbf{r}'_i = \mathbf{r}_i - \frac{1}{A} \sum_{j=1}^A \mathbf{r}_j$ , in order to take into account the center-of-mass correlations ( $\delta$  function in Eq. (10)). As was shown in [13], this leads to a one-particle nuclear density different from  $\rho_A$ . It should be noted that a one-particle nuclear density is different from a charge nuclear density measured in electron-nucleus scatterings. Thus, some cautions have to be undertaken at an extraction and a usage of nuclear parameters.

A systematical analysis of electron-nuclear data and a comparison with theoretical calculations (DHB approximation) have been done in paper [14] for an extraction of one-particle densities of nuclei. As a result, the densities were parameterized in the standard form:

$$\rho_A(r) = \frac{\rho_0}{1 + \exp\left(\frac{r - R_A}{d_A}\right)}, \quad R_A = 1.31A^{1/3} - 0.84 \text{ [fm]}, \quad d_A = 0.5 \text{ [fm]}. \quad (11)$$

The paper [14] is well-known in low- and intermediate-energy physics, especially in physics of exotic nuclei, because parameterizations of one-particle densities of protons and neutrons in nuclei were also presented in the paper.

The parameters of the distribution (11) have to be redefined in the following manner —  $R_A \rightarrow R_A \cdot A/(A-1)$ ,  $d_A \rightarrow d_A \cdot A/(A-1)$ , according to paper [13] for usage in Monte-Carlo calculations. In the case, a resulting density will coincide with  $\rho_A$  after the above-said redefinition of  $\mathbf{r}_i$ . We have used this prescription.

The shower enhancement coefficient was determined according to paper [15] as

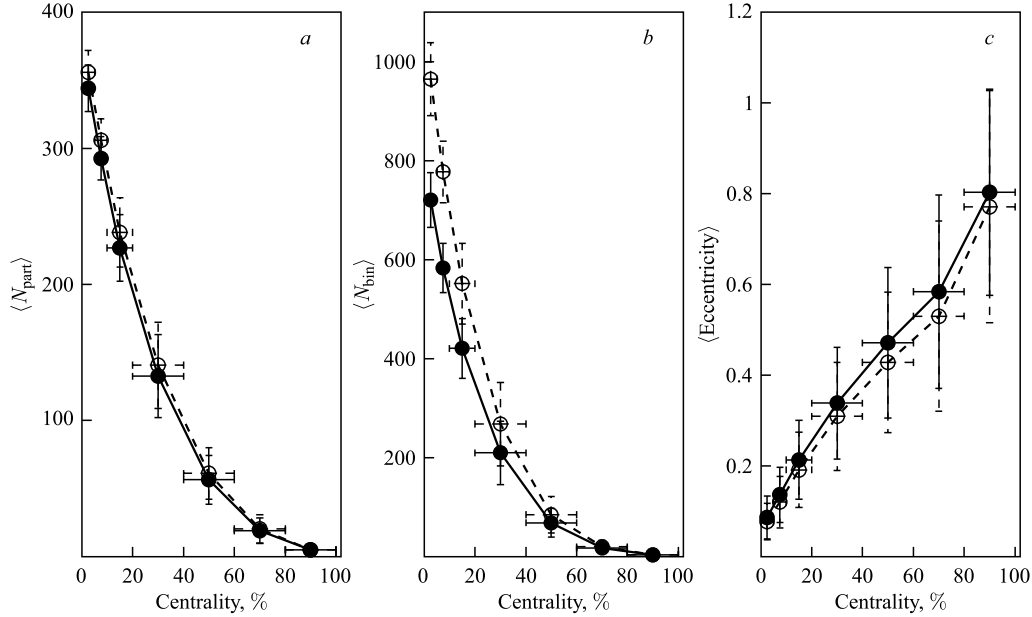
$$= 1.23 - 0.97/\sqrt{s}. \quad (12)$$

All specifications mentioned above were introduced in our Monte-Carlo program of the Glauber calculations. Results of calculations with the code are presented below.

Figure *a* shows dependencies of average multiplicities of the participating nucleons on a centrality of Au + Au collisions at  $\sqrt{s_{NN}} = 9$  and 200 GeV (closed and open points, respectively). Dispersions of the quantities are presented as “experimental error bars”. As seen, the multiplicities of the participating nucleons at low and high energies are differed in 3–5%. It is explained by the fact that high-energy collisions are differed from the low-energy one only due to larger radius of  $NN$  interactions from geometrical point of view. The radiuses are small compared with nuclear sizes. Though, the change of the radius at a transition from low to high energies has significant influence on the average multiplicities of the binary collisions (see Fig. *b*) and the anisotropy of nuclear interaction region (see Fig. *c*).

Usually, interactions of nuclei events are subdivided into the following centrality classes: 0–5, 5–10, 10–20, 20–40, 40–60, 60–80, 80–100% at experimental studies of superhigh energies. As seen in Figs. *a* and *b*, distributions on multiplicities of the participating nucleons and the binary collisions are inessential overlapping at high and low energies in neighboring intervals of the centrality at such subdivisions. Thus, the corresponding quantities for neighboring intervals —  $\langle N_{\text{part}} \rangle$  and  $\langle N_{\text{bin}} \rangle$  can be used for revelations of scaling properties of the interactions and the jet quenching in the collisions. Such applications become problematic at a more narrow interval subdivision due to a possible strong overlap of the distributions. As also seen, distributions on anisotropy of the interaction regions are strongly overlapping at all centrality classes (see Fig. *c*).

The anisotropy of the interaction region is characterized by the eccentricity in the last decade —  $\varepsilon_{\text{part}} = (\langle y^2 \rangle - \langle x^2 \rangle) / (\langle y^2 \rangle + \langle x^2 \rangle)$ , where  $x$  and  $y$  are coordinates of the



Mean multiplicities of the participating nucleons, binary collisions and the eccentricity as functions of the centrality (figures *a*, *b* and *c*, respectively). Dispersions of the quantities are presented as error bars

participating nucleon in the impact parameter plane counted from a center of the interaction region. We have used the definition in our calculations.  $\varepsilon_{part}$  in superhigh energy interactions is proportional to the magnitude of an elliptic flow, which is unambiguously connected with the properties of the quark–gluon plasma. One can expect a violation of the regularity and strong fluctuations of the collective flows at low energies and at an appearance of the mixed phase. Studies of such fluctuations are topics of modern experimental efforts of the last time.

The authors are grateful to B. V. Batyunya and G. Adam for stimulating discussions and interest in the work.

#### REFERENCES

1. Alver B. *et al.* arXiv:0805.4411 [nucl-exp]. 2005.
2. Miller M. L. *et al.* // Ann. Rev. Nucl. Part. Sci. 2007. V. 57. P. 205; arXiv:nucl-ex/0701025.
3. Kolb P. F., Heinz U. W. Quark–Gluon Plasma / Eds.: R. C. Hwa *et al.* SUNY-NTG-03-06. 2003. P. 634;  
Huovinen P. // Ibid. P. 600;  
Huovinen P., Ruuskanen P. V. // Ann. Rev. Nucl. Part. Sci. 2006. V. 56. P. 163;  
Gale C., Jeon S., Schenke B. arXiv:1301.5893 [nucl-th]. 2013.
4. Franco V. // Phys. Rev. 1968. V. 175. P. 1376;  
Czyz W., Maximon L. C. // Ann. Phys. (N. Y.). 1969. V. 52. P. 59;  
Kofod-Hansen O. // Nuovo Cim. A. 1969. V. 60. P. 621;  
Harrington D. R., Pagnamenta A. // Phys. Rev. 1969. V. 184. P. 1908;

- Formanek J.* // Nucl. Phys. B. 1969. V. 12. P. 441;  
*Alkhozov G. D., Belostotsky S. L., Vorobev A. A.* // Phys. Rep. 1978. V. 42. P. 89.
5. *Zadorozhnyi A. M., Uzhinsky V. V., Shmakov S. Yu.* // Sov. J. Nucl. Phys. 1984. V. 39. P. 729; *Yad. Fiz.* 1984. V. 39. P. 1155; JINR Preprint P2-83-544. Dubna, 1983.
  6. *Shmakov S. Yu., Uzhinskii V. V., Zadorozhny A. M.* // Comp. Phys. Commun. 1989. V. 54. P. 125.
  7. *Ding L.-K., Stenlund E.* // Comp. Phys. Commun. 1990. V. 59. P. 313.
  8. *Broniowski W., Rybczynski M., Bozek P.* // Comp. Phys. Commun. 2009. V. 180. P. 69.
  9. <http://root.cern.ch>
  10. *Uzhinsky V., Galoyan A.* // JETP Lett. 2011. V. 94. P. 499; *Pisma ZhETP.* 2011. V. 94. P. 539.
  11. *Uzhinsky V., Galoyan A.* arXiv:1111.4984 [hep-ph]. 2011.
  12. *Uzhinsky V., Galoyan A.* arXiv:1210.7338 [hep-ph]. 2012.
  13. *Uzhinsky V. V., Shmakov S. Yu.* // Phys. At. Nucl. 1994. V. 57. P. 1459; *Yad. Fiz.* 1994. V. 57. P. 1532.
  14. *Chamon L. C. et al.* // Phys. Rev. C. 2002. V. 66. P. 014610.
  15. *Uzhinsky V., Galoyan A.* // Phys. Lett. B. 2013. V. 721. P. 68.

Received on April 14, 2014.